Graphene Growth on and Transfer From Platinum Thin Films

Joon Hyong Cho
Mechanical Engineering Department,
The University of Texas at Austin,
Austin, TX 78712
e-mail: joonyboy@utexas.edu

Michael Cullinan[1]
Mechanical Engineering Department,
The University of Texas at Austin,
Austin, TX 78712
e-mail: michael.cullinan@austin.utexas.edu

This paper presents graphene growth on Pt thin films deposited with four different adhesion layers: Ti, Cr, Ta, and Ni. During the graphene growth at 1000 °C using conventional chemical vapor deposition (CVD) method, these adhesion layers diffuse into and alloy with Pt layer resulting in graphene to grown on different alloys. This means that each different adhesion layers induce a different quality and number of layer(s) of graphene grown on the Pt thin film. This paper presents the feasibility of graphene growth on Pt thin films with various adhesion layers and the obstacles needed to overcome in order to enhance graphene transfer from Pt thin films. Therefore, this paper addresses one of the major difficulties of graphene growth and transfer to the implementation of graphene in nano/micro-electromechanical systems (NEMS/MEMS) devices. [DOI: 10.1115/1.4038676]

Introduction

Graphene, a two-dimensional (2D) honeycomb lattice structure of sp^2-bonded carbon atoms, has gained enormous attention due to its exceptional mechanical and electrical characteristics [1]. Methods to produce graphene such as mechanical exfoliation from graphite [2], epitaxial growth on SiC [3], and chemical vapor deposition (CVD) on Ni thin film [4] are commonly used. However, for large-scale integration of graphene into devices, CVD growth is favorable since CVD-based fabrication can be done at the wafer scale by coating the entire wafer with a thin film of a transition metal such as Ru, Ir, Pt, Ni, and Cu. Each of the transition metals has a slightly varying mechanism for graphene growth since the carbon solubility, the active crystal facets, and the spacing between atoms are different for each transition metal [5]. The work in this paper focuses on the growth of graphene on Pt thin films due to the low carbon solubility and high thermal stability of platinum.

The direct integration of graphene into nano/micro-electromechanical systems (NEMS/MEMS) devices has many obstacles to overcome such as enhancing reliability and repeatability of graphene production at the wafer scale. The growth of high quality graphene is correlated to a complex set of relations between the substrate's surface roughness [6–8], lattice orientation [9,10], thermal stability at graphene growth temperature [11,12], number of defects and impurities present [13], and chemical inertness [7]. Therefore, the properties of the transition metal surface used to grow the graphene can have a large effect on the quality of graphene grown. Also, for transfer-free integration of graphene into NEMS/MEMS devices, the substrate metal film must be compatible to NEMS/MEMS fabrication processes [14]. This process is ideal for graphene-based device manufacturing [15], but problems with deweting of the thin films during growth raise issues with the direct growth of graphene onto the intended device wafer [16]. This paper investigates the possibilities of high-quality graphene growth on Pt thin films using four different adhesion layers to minimize dewetting and analyze the quality of graphene grown on Pt with each adhesion layer.

Background

Pt is known to have low adhesion to SiO_2 so the Pt layer can easily delaminate with a small external stress applied on the film. In order to have stable layer of Pt thin film on SiO_2/Si substrate, the addition of an adhesion layer is essential. We introduced four different adhesion layers, Ti, Cr, Ta, and Ni, to observe the effects of different adhesion layers on the growth of graphene on Pt thin films. Each of the four adhesion layers has different boiling points, thermal expansion coefficients, and alloying characteristics with Pt. These parameters are crucial to graphene growth which is done at 1000 °C in atmospheric pressure. At atmospheric pressure, boiling points of four adhesion layers are Ta (5731 K) > Ti (3560 K) > Ni (3003 K) > Cr (2944 K). Although these boiling points are far above graphene growth temperature at 1000 °C, atoms gain enough thermal energy at 1000 °C to become mobile and alloy with the Pt layer. Also, mobile atoms tend to agglomerate to reduce the surface energy of the film and this phenomenon occurs more severely on thinner thin films than thicker thin films which can be problematic for producing uniform graphene layers [5,11,12,17].

The thermal expansion coefficients of the four adhesion layers are Ni (13.4×10^{-6} K^{-1}) > Ti (8.6×10^{-6} K^{-1}) > Ta (6.3×10^{-6} K^{-1}) > Cr (4.9×10^{-6} K^{-1}). Metal surfaces tend to expand upon heating during the graphene growth and contract during the cool down after the growth. During the cycle, graphene and underlying substrate layers are under tensile and compressive strains. Thermal mismatch between these interlayers causes graphene to have wrinkles or cracks [18–20]. The adhesion layers' alloying characteristics with Pt are also important due to the fact that metal atoms from the adhesion layers diffuse into the Pt during the graphene growth at 1000 °C. Metals may or may not form perfect alloy and those different phases of alloys may or may not be favorable for graphene growth [5]. According to alloy phase diagrams of Pt–Ti, Pt–Cr, Pt–Ta, and Pt–Ni, only Ni adhesion layer favors mixing with Pt in homogenous form regardless of atomic weight ratio at 1000 °C [21]. Ni is a well-known layer to favor graphene growth due to its high carbon solubility [4]. In addition, monolayer graphene growth has been demonstrated on Ti and Ta thin films [22]. This paper demonstrates the effect of each of the four different adhesion layers on the growth graphene on Pt thin films.

Experiment

Adhesion layers, Ti, Cr, Ta, and Ni, each of 10 nm are deposited using e-beam evaporation. A 300-nm Pt thin film was deposited in the evaporator without breaking vacuum after the deposition of adhesion layers.

Atmospheric pressure CVD was used to grow the graphene without an annealing step to minimize dewetting of Pt thin film. In the atmospheric pressure CVD quartz chamber, 300 sccm of Ar was constantly flown as a carrier gas and temperature was ramped up to 1000 °C within 20 min. After the temperature reached 1000 °C, a 15% CH_4 (flow rate of CH_4 to H_2) gas mixture was introduced. Monolayer graphene growth was obtained with 3–5 min absorption time and multilayer graphene with 7.5–10 min absorption time.

A strong interaction between Pt and graphene reduces the Raman intensity hence analyzing graphene using Raman spectrum on Pt becomes a difficult task [10]. In order to avoid this issue,

[1]Corresponding author.
Contributed by the Manufacturing Engineering Division of ASME for publication in the JOURNAL OF MICRO- AND NANO-MANUFACTURING. Manuscript received September 27, 2017; final manuscript received November 21, 2017; published online December 26, 2017. Editor: Jian Cao.

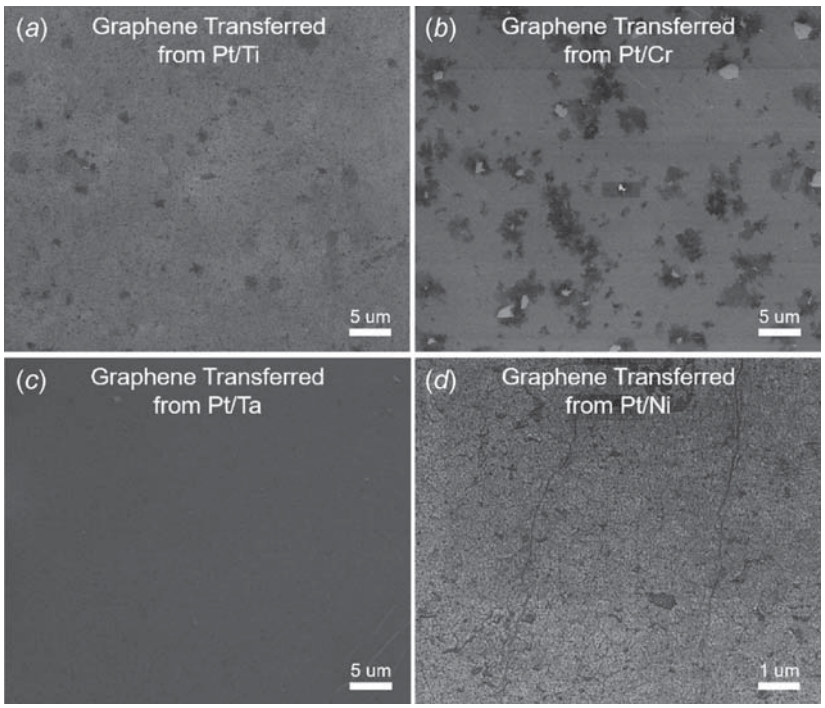

Fig. 1 Scanning electron microscopy (SEM) images of graphene transferred from Pt thin film with different adhesion layers: (*a*) Ti, (*b*) Cr, (*c*) Ta, and (*d*) Ni

graphene was transferred onto a Si substrate with a 300 nm SiO_2 layer. Both wet etch transfer and bubble transfer methods were used to find the best way to delaminate graphene from Pt thin films. For the wet etch transfer method, the graphene grown Pt thin film samples were spin-coated with polyvinylidene fluoride (PVDF) which is relatively resistant to Pt wet etchant and baked at 180 °C for 90 s to dry off the solvent. After spin-coating PVDF, the graphene/Pt samples were placed in a reduced nitric acid concentration Aqua Regia bath (a mixture of hydrochloric acid, nitric acid, de-ionized water in 6:1:1 ratio) for over 12 h. Afterward, the PVDF/graphene/SiO_2/Si samples were dried overnight in a desiccator. Polymer reflow was done by heating up dried sample on hot plate for 20 min at 180 °C to reduce graphene wrinkles and a warm acetone bath was used to remove PVDF for 8 h. The procedure for the bubble transfer process is given in Ref. [23].

Scanning electron microscopy (Quanta FEG 600) and Raman spectroscopy (Witec Micro-Raman Spectrometer Alpha 300, 488 nm Blue laser) were used to measure the overall coverage and number of graphene layers. Time-of-flight secondary ion mass spectrometry (TOF-SIMS, ION-TOF GmbH, Münster, Germany) was used to visualize the three-dimensional in-depth profile of graphene/Pt/adhesion-layer/SiO_2 interfaces.

Results

Wet etch transferred graphene on SiO_2/Si substrate from Pt thin film with four different adhesion layers of Ti, Cr, Ta, and Ni is observed with SEM images as shown in Figs. 1(*a*)–1(*d*). Graphene tears and holes are observable on all of the samples; however, graphene grown from Pt thin film with Cr adhesion layer has the largest number of holes and adlayers. Most of these holes are not from graphene transfer since adlayers are located around the holes. Adlayers tend to nucleate from defects or dislocations of metal grains or where facets are located [10]. It is likely that the defects or dislocations in this study were created during graphene growth at 1000 °C. This is supported by the fact that the Cr layer is the adhesion layer with the lowest melting point, and thus, it is the first adhesion layer to dewet. Dewetting of underlying layer will also affect the top morphology of Pt surface resulting in uniformity degradation of graphene during the growth.

Graphene from Pt/Ni thin film shows excessive wrinkles compared to other thin films. Observable wrinkles are due to induced thermal stresses during graphene growth and cooling. The Ni adhesion layer is the adhesion layer with the highest thermal expansion coefficient, and thus, is affected the most during the growth thermal stress cycle leaving the greatest number of wrinkles in the graphene. However, wrinkles are commonly caused while growing graphene on transition metals regardless of which adhesion layer is used due to difference between thermal expansion coefficients between the Pt and adhesion layers. Corrugated surfaces also tend to cause such wrinkles as reported in Ref. [18].

Figure 2 shows two SEM images of Pt grains on Cr and Ta adhesion layers after graphene growth. The Pt/Cr grains exhibit potential dewet holes, while the Pt/Ta grains remain stable over the wafer.

Characterization of the graphene is done by Raman spectroscopy as shown in Figs. 3(*a*)–3(*d*). The ratio of peak intensities of I_{2D} ($\approx$2690 cm^{-1}) over I_G ($\approx$1595 cm^{-1}) is used to reveal the number of graphene layers grown [24]. In most of the samples grown in this study, monolayer graphene was found ($I_{2D}/I_G \approx$ 1.8–2.5) except on graphene transferred from Pt/Ta thin films ($I_{2D}/I_G \approx$ 0.8–1.5). In addition, all of graphene transferred from Pt/Ti, Pt/Cr, and Pt/Ta exhibit D peak ($\approx$1350 cm^{-1}) where the presence of defects is found. Graphene transferred from Pt/Ni sample showed the smallest intensity of *D* peak which suggests that high-quality graphene growth on Pt/Ni is feasible.

The origin of the *D* peak on graphene is due to intrinsic and extrinsic factors. The use of graphene from Pt/Ti, Pt/Cr, and Pt/Ta can be ruled out for the implementation of graphene to NEMS/MEMS devices due to the presence of large defects as evidenced by the *D* peaks in these samples.

Figures 4(*a*) and 4(*b*) show the Pt surface after graphene transfer onto SiO_2/Si wafer indicating the lack of complete transfer and damage to the Pt surface. Two-dimensional Raman map and SEM

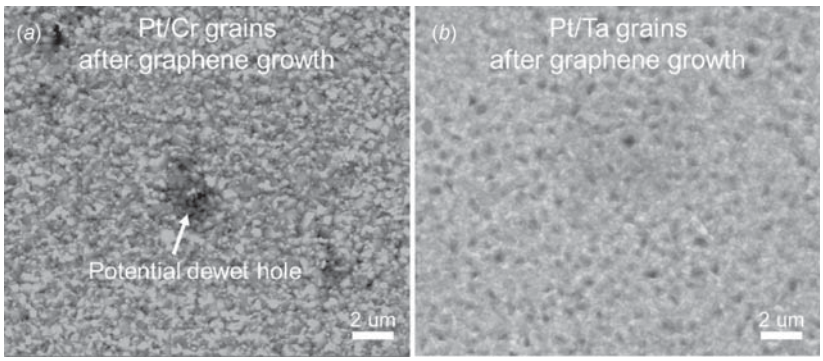

Fig. 2 Comparison of Pt grains with adhesion layers of the lowest boiling temperature (Cr) and of the highest boiling temperature (Ta). Arrow indicates the region where the potential dewet hole is present: (*a*) Pt/Cr grains after graphene growth and (*b*) Pt/Ta grains after graphene growth.

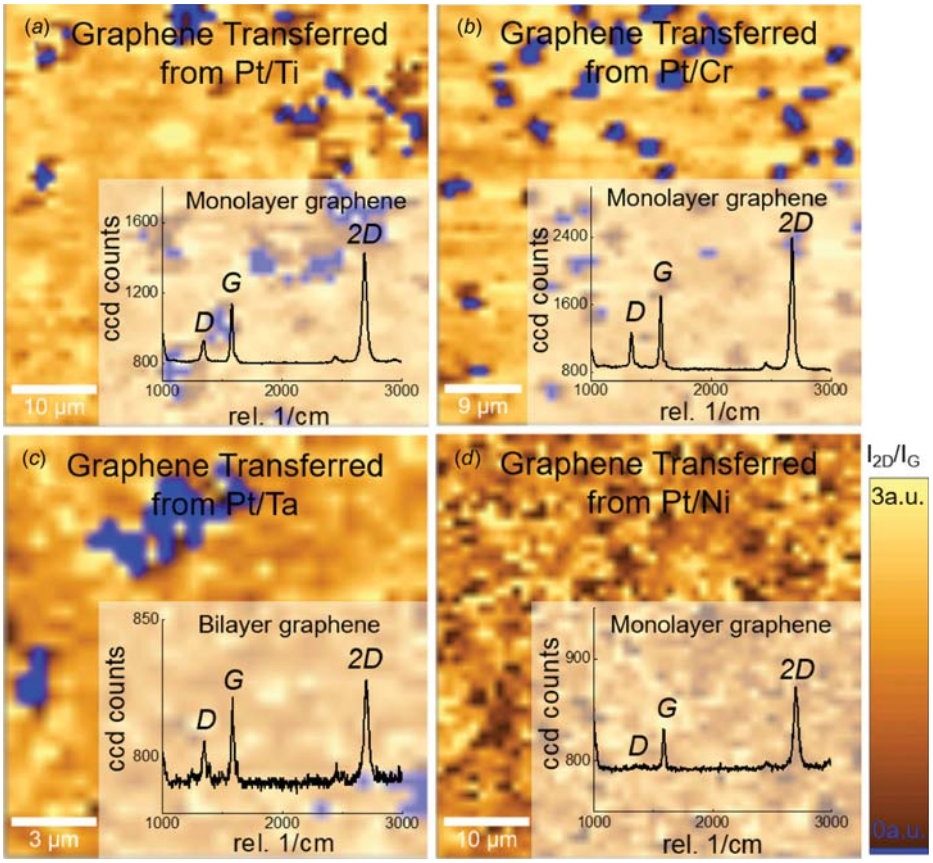

Fig. 3 Two-dimensional Raman maps of I2D peak over IG peak of graphene transferred from Pt thin film on adhesion layer of (*a*) Ti, (*b*) Cr, (*c*) Ta, and (*d*) Ni

images of graphene transferred using bubble transfer method also depict a lack of graphene uniformity after bubble transfer as shown in Figs. 4(*c*) and 4(*d*). The bubble transfer method on the Pt thin film required approximately 3–4 times longer time and two times higher bias voltage (7–12 V) to start the delamination process than is typically required for transfer from Pt foils [23]. This is likely due to nonuniform surface on the edge of Pt thin films where delamination must start, the nonuniformity of adhesion between graphene/Pt thin film along the surface, and the high electrical resistance compared to foils. Although the Poly(methyl methacrylate) (PMMA)/graphene layer was delaminated from Pt thin film, excessive bubbles from the transfer from thin films can attack graphene creating large cracks and tears across the surface. These cracks and tears were observed in all bubble transferred samples from Pt thin films regardless of type of adhesion layer used. Further research on why graphene transfer from Pt thin film is not favorable using bubble transfer must still be conducted.

For further analysis of interaction between Pt and adhesion layers, a TOF-SIMS analysis was performed. Figure 5(*a*) shows TOF-SIMS analysis of as deposited Pt/Ta thin film and Fig. 5(*b*) presents diffused Pt/Ta thin film after the graphene growth. Plus signs on each elements represent that an O_2 gun was used as a source for the measurements. Figure 5(*c*) shows the profile of an as deposited Pt/Ni sample and Fig. 5(*d*) shows Pt/Ni thin film

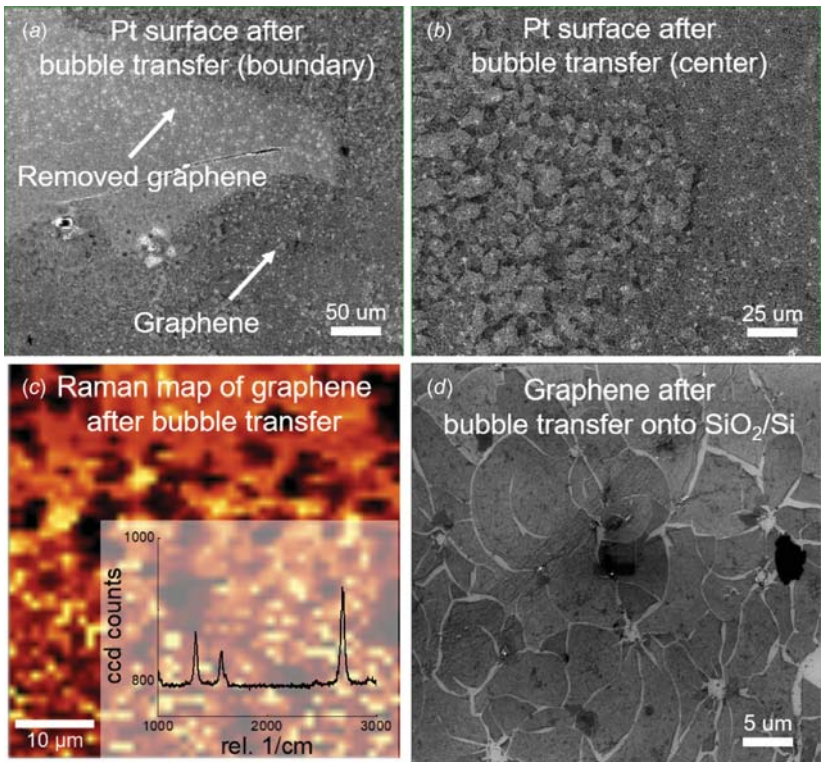

Fig. 4 SEM images of Pt surface after bubble transfer (*a*) in boundary and (*b*) center regions. (*c*) Two-dimensional Raman map of graphene transferred from Pt–Cr onto SiO_2/Si wafer using bubble transfer method. Both 2D Raman map (I_{2D}/I_G) and (*d*) a SEM image shows severely damaged condition of graphene due to hydrogen bubble impact during the transfer.

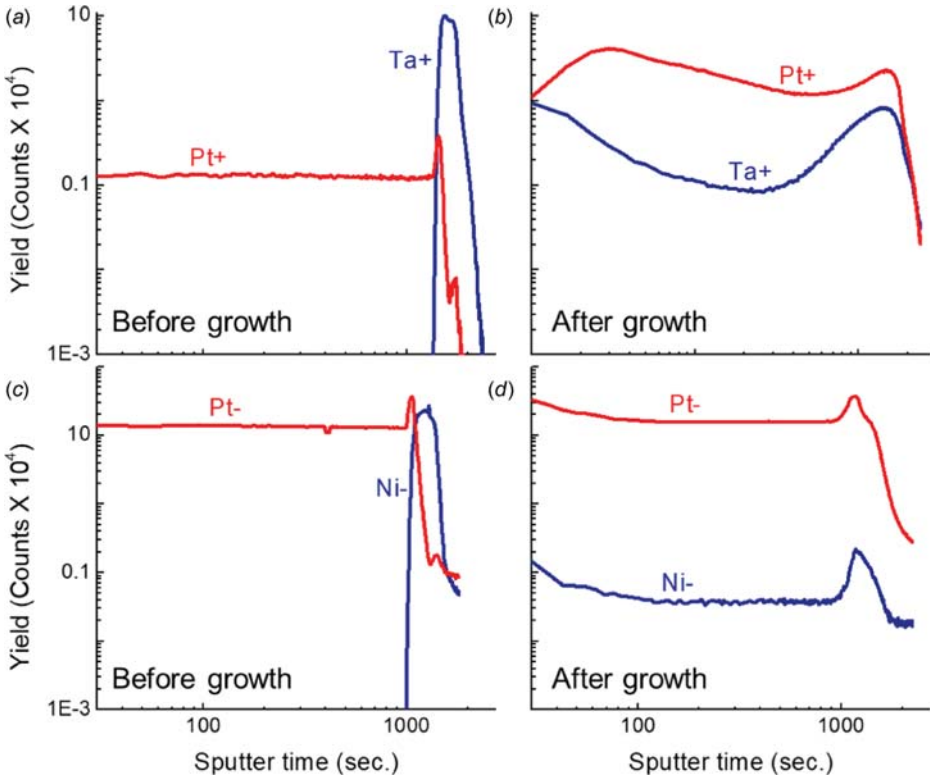

Fig. 5 TOF-SIMS analysis of two different adhesion layers: (*a*) Pt/Ta before graphene growth, (*b*) after graphene growth at 1000 °C, (*c*) Pt/Ni before graphene growth, and (*d*) after graphene growth at 1000 °C

sample with graphene grown on it. Negative signs on Pt and Ni elements indicate that a Cs source gun was used. The negative mode generally has higher power compared to positive mode hence sputtering time is shorter to reach 300 nm end point of Pt on the Pt/Ni samples than the Pt/Ta samples. Comparison between Figs. 5(*b*) and 5(*d*) depicts that Pt/Ni alloys homogenously throughout the whole film, where Pt/Ta thin film has nonuniform depth-profile which is consistent with the binary phase diagrams of these alloys [21]. Homogenous alloy of the film can be beneficial for uniform graphene growth since on an inhomogeneous phase surface graphene grows on distinct phases of surface which may cause the graphene to grow differently in different areas due to discrepancies in the local surface energy of the film. Therefore, inhomogeneous phase in the catalyst film is another potential barrier for uniform graphene growth over a large area.

Conclusions and Future Work

The low surface roughness, high thermal stability, chemical inertness, and controllable characteristics to configure number of graphene layers grown all make Pt thin films an excellent candidate for graphene growth. This paper demonstrates graphene growth on Pt thin film using four different adhesion layers and concludes that a good adhesion layer material requires high thermal stability as well as homogeneous mixing with Pt to promote graphene growth. Overall, the Ni adhesion layer is a promising candidate for graphene growth on thin film Pt due to these reasons. In addition, this paper demonstrates graphene transfer using PVDF in the replacement of conventional PMMA and shows that it is possible to transfer high quality graphene from Pt thin film using the wet etch method. Overall, this paper indicated that growth on thin film Pt is a promising route toward direct integration of graphene in NEMS/MEMS devices.

Acknowledgment

The authors would like to thank Dr. Alvin Lee for help with graphene growth, Dr. Andrei Dolocan for TOF-SIMS measurements, and Dr. Deji Akinwande and Dr. Richard Piner for their helpful discussions.

References

[1] Bunch, J. S., Van Der Zande, A. M., Verbridge, S. S., Frank, I. W., Tanenbaum, D. M., Parpia, J. M., Craighead, H. G., and Mceuen, P. L., 2007, "Electromechanical Resonators From Graphene Sheets," Science, **315**(5811), pp. 490–493.

[2] Novoselov, K. S., Geim, A. K., Morozov, S. V., Jiang, D., Zhang, Y., Dubonos, S. V., Grigorieva, I. V., and Firsov, A. A., 2004, "Electric Field Effect in Atomically Thin Carbon Films," Science, **306**(5696), pp. 666–669.

[3] Kedzierski, J., Hsu, P.-L., Healey, P., Wyatt, P. W., Keast, C. L., Sprinkle, M., Berger, C., and de Heer, W. A., 2008, "Epitaxial Graphene Transistors on SiC Substrates," IEEE Trans. Electron. Devices, **55**(8), pp. 2078–2085.

[4] Kim, K. S., Zhao, Y., Jang, H., Lee, S. Y., Kim, J. M., Ahn, J.-H., Kim, P., Choi, J.-Y., and Hong, B. H., 2009, "Large-Scale Pattern Growth of Graphene Films for Stretchable Transparent Electrodes," Nature, **457**(7230), pp. 706–710.

[5] Seah, C.-M., Chai, S.-P., and Mohamed, A. R., 2014, "Mechanisms of Graphene Growth by Chemical Vapour Deposition on Transition Metals," Carbon, **70**, pp. 1–21.

[6] Luo, Z., Lu, Y., Singer, D. W., Berck, M. E., Somers, L. A., Goldsmith, B. R., and Johnson, A. T. C., 2011, "Effect of Substrate Roughness and Feedstock Concentration on Growth of Wafer-Scale Graphene at Atmospheric Pressure," Chem. Mater., **23**(6), pp. 1441–1447.

[7] Kang, B. J., Mun, J. H., Hwang, C. Y., and Cho, B. J., 2009, "Monolayer Graphene Growth on Sputtered Thin Film Platinum," J. Appl. Phys., **106**(10), p. 104309.

[8] Lee, K., and Ye, J., 2016, "Significantly Improved Thickness Uniformity of Graphene Monolayers Grown by Chemical Vapor Deposition by Texture and Morphology Control of the Copper Foil Substrate," Carbon, **100**, pp. 441–449.

[9] Tao, L., Lee, J., Chou, H., Holt, M., Ruoff, R. S., and Akinwande, D., 2012, "Synthesis of High Quality Monolayer Graphene at Reduced Temperature on Hydrogen-Enriched Evaporated Copper (111) Films," ACS Nano, **6**(3), pp. 2319–2325.

[10] Gao, J.-H., Sagisaka, K., Kitahara, M., Xu, M.-S., Miyamoto, S., and Fujita, D., 2012, "Graphene Growth on a Pt(111) Substrate by Surface Segregation and Precipitation," Nanotechnology, **23**(5), p. 55704.

[11] Thompson, C. V., 2012, "Solid-State Dewetting of Thin Films," Annu. Rev. Mater. Res., **42**(1), pp. 399–434.

[12] Ismach, A., Druzgalski, C., Penwell, S., Schwartzberg, A., Zheng, M., Javey, A., Bokor, J., and Zhang, Y., 2010, "Direct Chemical Vapor Deposition of Graphene on Dielectric Surfaces," Nano Lett., **10**(5), pp. 1542–1548.

[13] Hao, Y., Wang, L., Liu, Y., Chen, H., Wang, X., Tan, C., Nie, S., Suk, J. W., Jiang, T., Liang, T., Xiao, J., Ye, W., Dean, C. R., Yakobson, B. I., Mccarty, K. F., Kim, P., Hone, J., Colombo, L., and Ruoff, R. S., 2016, "Oxygen-Activated Growth and Bandgap Tunability of Large Single-Crystal Bilayer Graphene," Nat. Nanotechnol., **11**(5), pp. 426–431.

[14] Cho, J. H., Sun, G., and Cullinan, M., 2016, "A Method to Manufacture Repeatable Graphene-Based NEMS Devices at the Wafer-Scale," ASME Paper No. MSEC2016-8567.

[15] Levendorf, M., Ruiz-Vargas, C., Garg, S., and Park, J., 2009, "Transfer-Free Batch Fabrication of Single Layer Graphene Transistors," Nano Lett., **9**(12), pp. 4479–4483.

[16] Cullinan, M. A., and Gorman, J. J., 2013, "Transfer-Free, Wafer-Scale Fabrication of Graphene-Based Nanoelectromechanical Resonators," Microsystems for Measurement and Instrumentation (MAMNA), Gaithersburg, MD, May 14, pp. 3–6.

[17] Nam, J., Kim, D.-C., Yun, H., Shin, D. H., Nam, S., Lee, W. K., Hwang, J. Y., Lee, S. W., Weman, H., and Kim, K. S., 2016, "Chemical Vapor Deposition of Graphene on Platinum: Growth and Substrate Interaction," Carbon, **111**, pp. 733–740.

[18] Gao, T., Xie, S., Gao, Y., Liu, M., Chen, Y., Zhang, Y., and Liu, Z., 2011, "Growth and Atomic-Scale Characterizations of Graphene on Multifaceted Textured Pt Foils Prepared by Chemical Vapor Deposition," ACS Nano, **5**(11), pp. 9194–9201.

[19] Shivaraman, S., Barton, R. A., Yu, X., Alden, J., Herman, L., Chandrashekhar, M. S. V., Park, J., McEuen, P. L., Parpia, J. M., Craighead, H. G., and Spencer, M. G., 2009, "Free-Standing Epitaxial Graphene," Nano Lett., **9**(9), pp. 3100–3105.

[20] Kang, J. H., Moon, J., Kim, D. J., Kim, Y., Jo, I., Jeon, C., Lee, J., and Hong, B. H., 2016, "Strain Relaxation of Graphene Layers by Cu Surface Roughening," Nano Lett., **16**(10), pp. 5993–5998.

[21] Okamoto, H., 2010, "Ni-Pt (Nickel-Platinum)," J. Phase Equilibria Diffus., **31**(3), p. 322.

[22] Soldano, C., Mahmood, A., and Dujardin, E., 2010, "Production, Properties and Potential of Graphene," Carbons, **48**(8), pp. 2127–2150.

[23] Gao, L., Ren, W., Xu, H., Jin, L., Wang, Z., Ma, T., Ma, L.-P., Zhang, Z., Fu, Q., Peng, L.-M., Bao, X., and Cheng, H.-M., 2012, "Repeated Growth and Bubbling Transfer of Graphene With Millimetre-Size Single-Crystal Grains Using Platinum," Nat. Commun., **3**, p. 699.

[24] Graf, D., Molitor, F., Ensslin, K., Stampfer, C., Jungen, A., Hierold, C., and Wirtz, L., 2007, "Spatially Resolved Raman Spectroscopy of Single- and Few-Layer Graphene," Nano Lett., **7**(2), pp. 238–242.